

MULTI-ALGORITHMIC METHODS FOR COUPLED HYPERBOLIC-PARABOLIC PROBLEMS

ALEXANDRE ERN AND JENNIFER PROFT

(Communicated by Peter Minev)

Abstract. We study computational methods for linear, degenerate advection-diffusion equations leading to coupled hyperbolic-parabolic problems. A multi-algorithmic approach is proposed in which a different approximation method is used locally depending on the mathematical nature of the problem. Our analysis focuses on stability and a priori error estimates of coupled continuous and discontinuous Galerkin methods, achieving a global $h^{p+\frac{1}{2}}$ estimate. Both the mathematical analysis and the numerical results demonstrate that careful consideration is necessary when defining appropriate interface conditions between the hyperbolic and parabolic regions.

Key Words. discontinuous Galerkin, NIPG, interface conditions, porous media, coupled hyperbolic/parabolic PDE's.

1. Introduction

This work is motivated by the study of flow and transport phenomena in highly heterogeneous porous media, an important application in the petroleum and environmental industries. An appealing technique for handling such phenomena is the use of a multi-algorithmic strategy based on the decomposition of the spatial domain into multiple non-overlapping subdomains according to the geological, physical and chemical properties of the medium. This promotes the use of a different scheme within each subdomain in order to reduce computational expenses while preserving accuracy. The resulting numerical models are consistent with the underlying equations on the subdomains and physically meaningful conditions are imposed on interfaces between the subdomains. Examples of such domain decomposition approaches include the mortar finite element method employing Lagrange multipliers to weakly impose flux-matching across interfaces [1, 2] and related multi-block multi-physics techniques [3, 4].

We consider the specific case of advective-diffusive transport of a chemical species within strongly contrasting geological layers where the resulting diffusion coefficient varies spatially. As a model problem, we investigate advection-diffusion equations where diffusion is locally degenerate within the computational domain, leading to a coupled hyperbolic-parabolic problem. This situation lends itself to the use of domain-decomposition type coupled continuous Galerkin (CG) and discontinuous Galerkin (DG) methods where the strengths of each method are exploited within

Received by the editors January 1, 2004 and, in revised form, March 22, 2005.

2000 *Mathematics Subject Classification.* 35R35, 35N .

This research was partially supported by GdR MoMaS (CNRS-2439, ANDRA, BRGM, CEA, EdF).

the appropriate subdomain. DG methods possess several characteristics which render them useful in many applications. Some well known versions include the local discontinuous Galerkin method of Cockburn and Shu [5], the OBB method of Oden, Babuška and Baumann [6], and the non-symmetric interior penalty Galerkin (NIPG) method of Rivière, Wheeler and Girault [7]. DG methods can efficiently handle advection-dominated flows since they generally exhibit less numerical diffusion than traditional CG methods, which efficiently handle diffusion-dominated flows. Furthermore the flexibility of DG methods allows for varying polynomial degree approximation and general non-conforming meshes. However, DG methods are more computationally expensive than CG methods since the degrees of freedom are associated with the elements rather than with the nodes. Thus, the use of a DG method on the hyperbolic subdomain coupled to a CG method on the parabolic region seems a natural choice.

When dealing with coupled hyperbolic-parabolic problems, special consideration must be paid to the interface conditions between parabolic and hyperbolic regions. For linear hyperbolic-parabolic problems such as those considered in this work, the interface conditions are relatively well understood. Gastaldi and Quarteroni [8] use a vanishing viscosity singular perturbation analysis to derive interface conditions for coupled hyperbolic-parabolic problems, which we employ henceforth. While the normal component of the total advective-diffusive flux is always continuous across the interface to ensure mass conservation, this is not the case for the solution itself. The latter is indeed continuous only at the subset of the interface where the flow leaves the parabolic subdomain and enters the hyperbolic region. On the other part of the interface, the solution is in general discontinuous. Recently, Croisille et al. [9] have used these interface conditions in the framework of the evolution linear semi-groups theory to establish a well-posedness result for one-dimensional, periodic, degenerate advection-diffusion equations.

In the case of a non-degenerate spatially-dependent diffusion coefficient yielding both advection-dominated and diffusion-dominated subdomains, it may be more useful to employ a DG method everywhere in the domain. A cost-effective strategy is to use, for instance, an NIPG method in the diffusion-dominated subdomain and a DG method in the advection-dominated subdomain. However, it remains important to be aware of the theoretical interface conditions when the Peclet number is sufficiently small to locally impose hyperbolic-type behavior in the solution. To pinpoint the main mathematical issues in this situation, we analyze a coupled NIPG/DG method for hyperbolic/parabolic problems.

This paper is organized as follows. The subsequent section defines the hyperbolic-parabolic problem and interface conditions under consideration. Section three analyzes a coupled CG/DG method and presents some convergence results as well as numerical results obtained with the coupled scheme on a model problem. Motivated by this approach and the careful treatment of terms in the resulting discretizations arising on the interface, section four then considers a scheme coupling the NIPG method in the parabolic subdomain with the DG method in the hyperbolic subdomain. The coupled NIPG/DG scheme is analyzed and convergence results are presented. In particular, we emphasize the fact that special consideration should be devoted to the design of interface conditions. The numerical results demonstrate that this difficulty must be tackled even in fully parabolic problems at the interface of those subdomains where the diffusion is dominated by the advection term, a difficult problem reflective of the small Peclet number associated with the equation. Conclusions are drawn in section five.

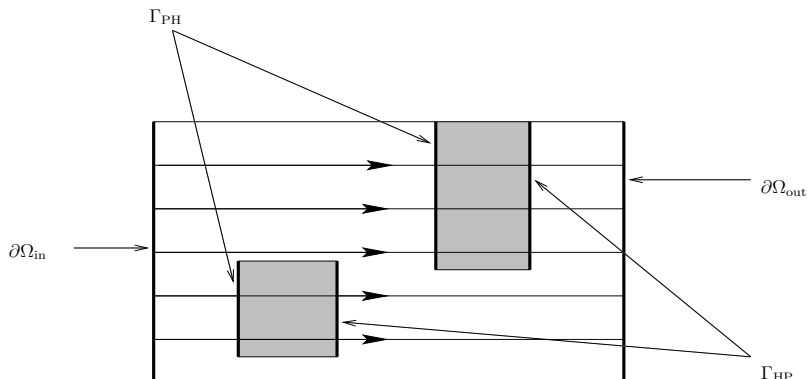


FIGURE 1. Domain decomposition setting for the coupled hyperbolic-parabolic problem; Ω is a rectangle, Ω_H is shown in gray, and Ω_P is the complement of Ω_H . In this example, the flow lines are horizontal.

2. The setting

This section describes the model problem and presents some notation and analysis tools.

2.1. Problem definition. Consider the degenerate advection-diffusion equation

$$\begin{aligned} (1) \quad & \partial_t u + \nabla \cdot (\alpha u - \nu \nabla u) = 0, & x \in \Omega_P, t \geq 0, \\ (2) \quad & \partial_t u + \nabla \cdot (\alpha u) = 0, & x \in \Omega_H, t \geq 0, \end{aligned}$$

defined on two distinct subdomains of bounded polygonal domain Ω in \mathbb{R}^d , $d = 1, 2, 3$, divided into parabolic region Ω_P and hyperbolic region Ω_H with internal interface $\Gamma = \partial\Omega_P \cap \partial\Omega_H$. We assume that the diffusion tensor ν is symmetric positive definite and bounded in Ω_P uniformly from above and below by a positive constant. We also assume that the velocity field α is time-independent and that it is in $W_\infty^1(\Omega)$ and satisfies the continuity equation $\nabla \cdot \alpha = 0$. Let $n_{\partial\Omega}$ be the unit outward normal to domain boundary $\partial\Omega$. Define inflow region $\partial\Omega_{\text{in}} = \{x \in \partial\Omega : \alpha \cdot n_{\partial\Omega} < 0\}$, non-slip region $\partial\Omega_0 = \{x \in \partial\Omega : \alpha \cdot n_{\partial\Omega} = 0\}$, and outflow region $\partial\Omega_{\text{out}} = \{x \in \partial\Omega : \alpha \cdot n_{\partial\Omega} > 0\}$. We assume for simplicity that the inflow and outflow portions exist on the parabolic domain only, i.e., that $\partial\Omega_H \cap \partial\Omega_{\text{in}} = \partial\Omega_H \cap \partial\Omega_{\text{out}} = \emptyset$. Conventionally set the unit normal n_Γ on Γ to face outward from Ω_P and inward to Ω_H . Define the following subsets of interface Γ : $\Gamma_{PH} = \{x \in \Gamma : \alpha \cdot n_\Gamma > 0\}$ and $\Gamma_{HP} = \{x \in \Gamma : \alpha \cdot n_\Gamma < 0\}$, i.e., the flow crosses Γ_{PH} from the parabolic to the hyperbolic subdomain and vice versa across Γ_{HP} . The domain decomposition setting is illustrated in Figure 1.

Equations (1)-(2) are supplemented with initial and boundary conditions of the form

$$\begin{aligned} (3) \quad & u(x, t) = u_0(x), & x \in \Omega, t = 0, \\ (4) \quad & (\alpha u(x, t) - \nu \nabla u(x, t)) \cdot n_{\partial\Omega} = \alpha \hat{g}(x) \cdot n_{\partial\Omega}, & x \in \partial\Omega_{\text{in}}, t \geq 0, \\ (5) \quad & -\nu \nabla u(x, t) \cdot n_{\partial\Omega} = 0, & x \in \partial\Omega_{\text{out}} \cup \partial\Omega_0, t \geq 0, \end{aligned}$$

with $u_0 \in L^2(\Omega)$ and $\hat{g} \in L^2(\partial\Omega_{\text{in}})$. To complete the framework, interface conditions must be specified between the hyperbolic and parabolic subdomains. For

coupled hyperbolic-parabolic problems, careful consideration of valid interface conditions at the interface is crucial to deriving a well-posed problem; see Gastaldi and Quarteroni [8] and Croisille et al. [9]. Let u^P and u^H be the restriction of the solution to each respective subdomain. Then for parabolic to hyperbolic flow across Γ_{PH} , two interface conditions hold:

$$(6) \quad (\alpha u^P - \nu \nabla u^P) \cdot n_\Gamma = \alpha u^H \cdot n_\Gamma \quad \text{on } \Gamma_{PH},$$

$$(7) \quad \alpha u^P \cdot n_\Gamma = \alpha u^H \cdot n_\Gamma \quad \text{on } \Gamma_{PH},$$

while for hyperbolic to parabolic flow across Γ_{HP} , only one interface condition holds:

$$(8) \quad (\alpha u^P - \nu \nabla u^P) \cdot n_\Gamma = \alpha u^H \cdot n_\Gamma \quad \text{on } \Gamma_{HP}.$$

Note that (6)-(8) imply that the normal component of the total advective-diffusive flux is continuous throughout the domain. This is important to ensure mass conservation when the unknown u mimics a concentration. The degeneracy of the diffusion coefficient leads to discontinuous behavior in the solution or in its derivative. In particular, at the interface from parabolic to hyperbolic flow, the solution u is C^0 but exhibits a discontinuity in the normal derivative; in the reverse situation from hyperbolic to parabolic flow, the solution u exhibits a discontinuity. We also observe that conditions (3)-(4) are equivalent to imposing the continuity of the solution across Γ_{PH} and the usual homogeneous Neumann outflow condition on u^P .

In what follows we assume that the model problem (1)-(8) admits a strong solution u in the sense that u is continuous on $\bar{\Omega} \setminus \Gamma_{HP}$ and that the PDE's (1)-(2), the initial and boundary conditions (3)-(5) and the interface conditions (6)-(8) are satisfied a.e. in time and space.

2.2. Notational preliminaries. Let $\{\mathcal{T}_h\}_{h>0}$ denote a shape-regular family of finite element subdivisions of domain Ω partitioned into open disjoint elements Ω_e . Assume that the meshes \mathcal{T}_h are compatible with the partitioning of Ω into Ω_P and Ω_H . Let $\mathcal{T}_h(\Omega_P)$ and $\mathcal{T}_h(\Omega_H)$ denote the set of mesh elements in Ω_P and Ω_H , respectively. Let F_h be the set of faces belonging to elements $\Omega_e \in \mathcal{T}_h$ and partition F_h into distinct sets $F^i \cup F_{\text{in}}^\partial \cup F_0^\partial \cup F_{\text{out}}^\partial$, where F^i denotes the set of interior faces, F_{in}^∂ the set of faces located on $\partial\Omega_{\text{in}}$, F_0^∂ the set of faces located on $\partial\Omega_0$, and F_{out}^∂ the set of faces located on $\partial\Omega_{\text{out}}$. Let the set of interior faces be further divided into distinct sets $F^i = F_P^i \cup F_H^i \cup F_\Gamma^i$, where F_P^i denotes the set of interior faces restricted to subdomain Ω_P , F_H^i the set of interior faces restricted to subdomain Ω_H , and F_Γ^i the set of interior faces on interface Γ . We assume that the mesh is compatible with the partitioning of the boundary $\partial\Omega$ and that of interface Γ ; in particular, we assume that a face $F \in F_\Gamma^i$ is entirely located either in Γ_{PH} , or in Γ_{HP} , or in neither of these two sets. For an interior face $F \in F^i$ shared by elements Ω_{e1} and Ω_{e2} with respective unit outward normals n_1 and n_2 and for a function v with restrictions $v_1 = v|_{\Omega_{e1}}$ and $v_2 = v|_{\Omega_{e2}}$ that are smooth enough, define the average and (vector-valued) jump of v as

$$(9) \quad \{v\}_F = \frac{1}{2}(v_1 + v_2) \quad \text{and} \quad [v]_F = v_1 n_1 + v_2 n_2,$$

respectively. Assuming that $\alpha \cdot n_1 \neq 0$, define the upwind value

$$(10) \quad v_F^\uparrow = v_1 1_{\{\alpha \cdot n_1 \geq 0\}} + v_2 1_{\{\alpha \cdot n_2 > 0\}}.$$

When no confusion may arise, the subscript F is dropped in (9)-(10). Finally, letting $n_F = \pm n_1$, $|\alpha \cdot n_F|$ denotes the absolute value of the normal component of α across F .

Let $H^s(\Omega)$ denote the standard Sobolev space equipped with the usual norm $\|\cdot\|_{H^s(\Omega)}$. Let $H^s(\mathcal{T}_h)$ denote the space of functions whose restriction to the elements $\Omega_e \in \mathcal{T}_h$ is in $H^s(\Omega_e)$. For a time-space function u , the notation $u \in L_t^2(H_x^s)$ (resp. $u \in C_t^k(H_x^s)$) means that the function $(0, T) \ni t \mapsto u(t, \cdot) \in H^2(\Omega)$ is in $L^2(0, T)$ (resp. $C^k(0, T)$) where T is a fixed time. We will use the standard L^2 inner product notation $(\cdot, \cdot)_R$ for domains $R \subset \mathbb{R}^d$, and the notation $\langle \cdot, \cdot \rangle_F$ to denote integration over a face F of the mesh.

2.3. Analysis Tools. In our analysis, we use the following well-known trace inequality [10]: Suppose that element Ω_e has a Lipschitz boundary. Then, there is a constant C_e^t such that

$$(11) \quad \|v\|_{L^2(\partial\Omega_e)} \leq C_e^t \|v\|_{L^2(\Omega_e)}^{\frac{1}{2}} \|v\|_{H^1(\Omega_e)}^{\frac{1}{2}} \quad \forall v \in H^1(\Omega_e).$$

Define the trace constant $C_t = \max_{\Omega_e \in \mathcal{T}_h} C_e^t$ and assume that $\{\mathcal{T}_h\}_{h>0}$ is such that C_t can be bounded by a finite constant uniformly in h .

For a positive integer p and a mesh element $\Omega_e \in \mathcal{T}_h$, define $\mathbb{P}^p(\Omega_e)$ to be the set of polynomials of degree less than or equal to p on Ω_e . We will have occasion to use a standard inverse inequality, valid for piecewise polynomials on shape-regular families of triangulations [10, 11]: There exists a constant C_i independent of Ω_e such that

$$(12) \quad \|v\|_{H^1(\Omega_e)} \leq C_i h_e^{-1} \|v\|_{\Omega_e} \quad \forall v \in \mathbb{P}^p(\Omega_e),$$

where $h_e = \text{diam}(\Omega_e)$. Recall the standard h approximation properties: For L^2 -orthogonal projection $\Pi^0 v$ of $v \in H^k(\Omega_e)$ onto $\mathbb{P}^p(\Omega_e)$, there exists a constant C_a independent of h_e such that

$$(13) \quad \|v - \Pi^0 v\|_{H^q(\Omega_e)} \leq C_a h_e^{\mu-q} \|v\|_{H^k(\Omega_e)}, \quad 0 \leq k \leq p+1,$$

where $\mu = \min(p+1, k)$ and $0 \leq q \leq \mu$.

We will have occasion to use the following form of Gronwall's lemma [10]: Let g and ρ be piecewise continuous non-negative functions defined on an interval $a \leq t \leq b$, ρ being also non-decreasing. If for $t \in [0, b]$, $g(t) + h(t) \leq \rho(t) + \int_a^t g(s) ds$, then $g(t) + h(t) \leq C\rho(t)$ with $C = \exp(t-a)$. Additionally, Young's inequality will prove useful in our analysis: For real numbers a, b and for $\delta > 0$, $2ab \leq \delta a^2 + \delta^{-1} b^2$.

3. Coupled CG/DG formulation

In this section we formulate the coupling of the CG method discretizing the parabolic equation (1) on Ω_P with the DG method discretizing the hyperbolic equation (2) on Ω_H . Then, we analyze the consistency, stability, and convergence properties of the resulting scheme. Finally, we present some numerical results.

3.1. The scheme. Let p_{CG} and p_{DG} be two positive integers and define the finite element spaces

$$(14) \quad V_h^{CG} = \{v \in C^0(\overline{\Omega_P}) : \forall \Omega_e \in \mathcal{T}_h(\Omega_P), v|_{\Omega_e} \in \mathbb{P}^{p_{CG}}(\Omega_e)\},$$

$$(15) \quad V_h^{DG} = \{v \in L^2(\Omega_H) : \forall \Omega_e \in \mathcal{T}_h(\Omega_H), v|_{\Omega_e} \in \mathbb{P}^{p_{DG}}(\Omega_e)\}.$$

For a smooth enough function ψ , set $\psi^P = \psi|_{\Omega_P}$ and $\psi^H = \psi|_{\Omega_H}$. For test functions $w_h \in V_h^{CG}$ and $v_h \in V_h^{DG}$, define the bilinear forms

$$(16) \quad \begin{aligned} a_{CG}(\psi, w_h) &= (\partial_t \psi^P, w_h)_{\Omega_P} - (\alpha \psi^P - \nu \nabla \psi^P, \nabla w_h)_{\Omega_P} \\ &+ \sum_{F \in F_\Gamma^i} \langle \alpha \psi^\uparrow \cdot n_\Gamma, w_h \rangle_F + \sum_{F \in F_{\text{out}}^\partial} \langle \alpha \psi^P \cdot n_{\partial\Omega}, w_h \rangle_F, \end{aligned}$$

$$(17) \quad \begin{aligned} a_{DG}(\psi, v_h) &= (\partial_t \psi^H, v_h)_{\Omega_H} - \sum_{\Omega_e \in \mathcal{T}_h(\Omega_H)} (\alpha \psi^H, \nabla v_h)_{\Omega_e} \\ &- \sum_{F \in F_\Gamma^i} \langle \alpha \psi^\uparrow \cdot n_\Gamma, v_h \rangle_F + \sum_{F \in F_H^i} \langle \alpha (\psi^H)^\uparrow, [v_h] \rangle_F, \end{aligned}$$

and the linear form

$$(18) \quad l_{CG}(w_h) = - \sum_{F \in F_{\text{in}}^\partial} \langle \alpha \hat{g} \cdot n_{\partial\Omega}, w_h \rangle_F.$$

In (16)-(17), the left argument of a_{CG} and a_{DG} is ψ and not ψ^P or ψ^H , respectively, owing to the presence of the upwind term at the interface Γ .

To approximate the solution of (1)-(8), consider the following coupled continuous-discontinuous discrete formulation: Seek $u_h = (u_h^P, u_h^H) \in C^1([0, T]; V_h^{CG} \times V_h^{DG})$ such that, for all $t > 0$,

$$(19) \quad a_{CG}(u_h, w_h) + a_{DG}(u_h, v_h) = l_{CG}(w_h) \quad \forall (w_h, v_h) \in V_h^{CG} \times V_h^{DG},$$

and at $t = 0$ define $u_h(0) = (u_h^P(0), u_h^H(0)) \in V_h^{CG} \times V_h^{DG}$ to be the L^2 -orthogonal projection of u_0 onto $V_h^{CG} \times V_h^{DG}$,

$$(20) \quad (u_h^P(0) - u_0, v_h)_{\Omega_P} + (u_h^H(0) - u_0, w_h)_{\Omega_H} = 0 \quad \forall (v_h, w_h) \in V_h^{CG} \times V_h^{DG}.$$

3.2. Analysis. To prove the convergence of u_h , the solution of (19)-(20), to the solution of (1)-(8), we establish consistency, stability, and approximability properties for the coupled continuous/discontinuous formulation (19).

Lemma 3.1 (consistency). *Assume that u is a strong solution of (1)-(8). Then,*

$$(21) \quad a_{CG}(u, w_h) + a_{DG}(u, v_h) = l_{CG}(w_h) \quad \forall (w_h, v_h) \in V_h^{CG} \times V_h^{DG}.$$

Proof. The key point consists of verifying that the upwind terms in (16) and (17) yield the correct advective-diffusive flux on faces $F \in F_\Gamma^i$. Let $F \subset \Gamma_{PH}$. Then, $u^\uparrow = u^P$, and using (6)-(7) yields

$$(22) \quad \alpha u^\uparrow \cdot n_\Gamma = \alpha u^P \cdot n_\Gamma = \alpha u^H \cdot n_\Gamma = (\alpha u^P - \nu \nabla u^P) \cdot n_\Gamma.$$

In the case $F \subset \Gamma_{HP}$, $u^\uparrow = u^H$, yielding

$$(23) \quad \alpha u^\uparrow \cdot n_\Gamma = \alpha u^H \cdot n_\Gamma = (\alpha u^P - \nu \nabla u^P) \cdot n_\Gamma.$$

Hence, in both cases, $\alpha u^\uparrow \cdot n_\Gamma$ equals the value of the advective-diffusive flux on Γ . To verify equation (21), integrate by parts the terms involving test function gradients in (16)-(17). The conclusion follows easily. \square

Define the norm

$$\begin{aligned}
|||\psi|||^2 &\equiv \frac{1}{2} \|\psi(T)\|_{\Omega}^2 + \int_0^T \|\nu^{\frac{1}{2}} \nabla \psi^P\|_{\Omega_P}^2 \\
&\quad + \frac{1}{2} \int_0^T \sum_{F \in F_{\text{out}}^{\partial}} \langle |\alpha \cdot n_{\partial\Omega}|, (\psi^P)^2 \rangle_F + \frac{1}{2} \int_0^T \sum_{F \in F_{\text{in}}^{\partial}} \langle |\alpha \cdot n_{\partial\Omega}|, (\psi^P)^2 \rangle_F \\
(24) \quad &\quad + \frac{1}{2} \int_0^T \sum_{F \in F_{\text{H}}^i} \langle |\alpha \cdot n_F|, [\psi^H]^2 \rangle_F + \frac{1}{2} \int_0^T \sum_{F \in F_{\Gamma}^i} \langle |\alpha \cdot n_{\Gamma}|, [\psi]^2 \rangle_F.
\end{aligned}$$

Lemma 3.2 (stability). *The following identity holds: For all $v_h = (v_h^P, v_h^H) \in V_h^{\text{CG}} \times V_h^{\text{DG}}$,*

$$(25) \quad \int_0^T a_{\text{CG}}(v_h, v_h^P) + \int_0^T a_{\text{DG}}(v_h, v_h^H) = |||v_h|||^2 - \frac{1}{2} \|v_h(0)\|_{\Omega}^2.$$

Proof. Let $v_h \in V_h^{\text{CG}} \times V_h^{\text{DG}}$. The following terms are easily rewritten as

$$(26) \quad \int_0^T (\partial_t v_h^P, v_h^P)_{\Omega_P} + \int_0^T (\partial_t v_h^H, v_h^H)_{\Omega_H} = \frac{1}{2} \|v_h(T)\|_{\Omega}^2 - \frac{1}{2} \|v_h(0)\|_{\Omega}^2,$$

and

$$(27) \quad \int_0^T (\nu \nabla v_h^P, \nabla v_h^P)_{\Omega_P} = \int_0^T \|\nu^{\frac{1}{2}} \nabla v_h^P\|_{\Omega_P}^2.$$

Furthermore,

$$\begin{aligned}
& - \int_0^T (\alpha v_h^P, \nabla v_h^P)_{\Omega_P} = -\frac{1}{2} \int_0^T (\alpha, \nabla (v_h^P)^2)_{\Omega_P} \\
& = -\frac{1}{2} \int_0^T \sum_{F \in F_{\text{out}}^{\partial}} \langle \alpha \cdot n_{\partial\Omega}, (v_h^P)^2 \rangle_F - \frac{1}{2} \int_0^T \sum_{F \in F_{\text{in}}^{\partial}} \langle \alpha \cdot n_{\partial\Omega}, (v_h^P)^2 \rangle_F \\
(28) \quad & - \frac{1}{2} \int_0^T \sum_{F \in F_{\Gamma}^i} \langle \alpha \cdot n_{\Gamma}, (v_h^P)^2 \rangle_F,
\end{aligned}$$

as well as

$$\begin{aligned}
(29) \quad & - \int_0^T \sum_{\Omega_e \in \mathcal{T}_h(\Omega_H)} (\alpha v_h^H, \nabla v_h^H)_{\Omega_e} = -\frac{1}{2} \int_0^T \sum_{\Omega_e \in \mathcal{T}_h(\Omega_H)} (\alpha, \nabla (v_h^H)^2)_{\Omega_e} \\
& = -\frac{1}{2} \int_0^T \sum_{F \in F_{\text{H}}^i} \langle \alpha, [(v_h^H)^2] \rangle_F + \frac{1}{2} \int_0^T \sum_{F \in F_{\Gamma}^i} \langle \alpha \cdot n_{\Gamma}, (v_h^H)^2 \rangle_F.
\end{aligned}$$

Using the definition of $\partial\Omega_{\text{in}}$ and $\partial\Omega_{\text{out}}$, the combined boundary terms can be written

$$\begin{aligned}
(30) \quad & \frac{1}{2} \int_0^T \sum_{F \in F_{\text{out}}^{\partial}} \langle \alpha \cdot n_{\partial\Omega}, (v_h^P)^2 \rangle_F - \frac{1}{2} \int_0^T \sum_{F \in F_{\text{in}}^{\partial}} \langle \alpha \cdot n_{\partial\Omega}, (v_h^P)^2 \rangle_F \\
& = \frac{1}{2} \int_0^T \sum_{F \in F_{\text{out}}^{\partial}} \langle |\alpha \cdot n_{\partial\Omega}|, (v_h^P)^2 \rangle_F + \frac{1}{2} \int_0^T \sum_{F \in F_{\text{in}}^{\partial}} \langle |\alpha \cdot n_{\partial\Omega}|, (v_h^P)^2 \rangle_F.
\end{aligned}$$

Let $F \in F_{\text{H}}^i$ be shared by elements Ω_{e1} and Ω_{e2} with respective unit outward normals n_1 and n_2 . Set $v_1 = v_h^H|_{\Omega_{e1}}$ and $v_2 = v_h^H|_{\Omega_{e2}}$. Assume $\alpha \cdot n_1 > 0$. Then, by

the definition of the upwind and jump values of a function,

$$\begin{aligned}
-\frac{1}{2}\alpha \cdot [v_h^H]^2 + \alpha(v_h^H)^\uparrow \cdot [v_h^H] &= -\frac{1}{2}\alpha \cdot (v_1^2 n_1 + v_2^2 n_2) + \alpha v_1 \cdot (v_1 n_1 + v_2 n_2) \\
&= \alpha \cdot n_1 (\frac{1}{2}v_1^2 + \frac{1}{2}v_2^2 - v_1 v_2) \\
(31) \qquad \qquad \qquad &= \frac{1}{2}|\alpha \cdot n_F|[v_h^H]^2.
\end{aligned}$$

The result also holds if $\alpha \cdot n_1 < 0$ and (trivially) if $\alpha \cdot n_1 = 0$. Hence,

$$\begin{aligned}
(32) \quad -\frac{1}{2} \int_0^T \sum_{F \in F_H^i} \langle \alpha, [(v_h^H)^2] \rangle_F + \int_0^T \sum_{F \in F_H^i} \langle \alpha(v_h^H)^\uparrow, [v_h^H] \rangle_F \\
= \frac{1}{2} \int_0^T \sum_{F \in F_H^i} \langle |\alpha \cdot n_F|, [v_h^H]^2 \rangle_F.
\end{aligned}$$

Let now $F \in F_\Gamma^i$ and use a similar notation as above with (for instance) Ω_{e1} located in Ω_P and Ω_{e2} in Ω_H so that $n_\Gamma = n_1 = -n_2$. Assume $\alpha \cdot n_1 > 0$. Then,

$$\begin{aligned}
-\frac{1}{2}\alpha(v_h^P)^2 \cdot n_\Gamma + \frac{1}{2}\alpha(v_h^H)^2 \cdot n_\Gamma + \alpha v_h^\uparrow \cdot [v_h] \\
= -\frac{1}{2}\alpha \cdot n_1 v_1^2 + \frac{1}{2}\alpha \cdot n_1 v_2^2 + \alpha v_1 (v_1 n_1 + v_2 n_2) \\
= \alpha \cdot n_1 (\frac{1}{2}v_1^2 + \frac{1}{2}v_2^2 - v_1 v_2) \\
(33) \qquad \qquad \qquad = \frac{1}{2}|\alpha \cdot n_F|[v_h]^2,
\end{aligned}$$

and the result also holds if $\alpha \cdot n_1 \leq 0$. Hence,

$$\begin{aligned}
(34) \quad -\frac{1}{2} \int_0^T \sum_{F \in F_\Gamma^i} \langle \alpha \cdot n_\Gamma, (v_h^P)^2 \rangle_F + \frac{1}{2} \int_0^T \sum_{F \in F_\Gamma^i} \langle \alpha \cdot n_\Gamma, (v_h^H)^2 \rangle_F \\
+ \int_0^T \sum_{F \in F_\Gamma^i} \langle \alpha v_h^\uparrow, [v_h] \rangle_F = \frac{1}{2} \int_0^T \sum_{F \in F_\Gamma^i} \langle |\alpha \cdot n_\Gamma|, [v_h]^2 \rangle_F.
\end{aligned}$$

Combining each of the above results yields the lemma. \square

Corollary 3.3. *The scheme (19)-(20) satisfies the stability result*

$$(35) \quad |||u_h|||^2 \leq \|u_0\|_\Omega^2 + 2 \int_0^T \sum_{F \in F_{in}^o} \langle |\alpha \cdot n_{\partial\Omega}|, \hat{g}^2 \rangle_F.$$

Proof. Take $w = u_h^P$ and $v = u_h^H$ in (19) and integrate in time from 0 to T to obtain

$$(36) \quad \int_0^T a_{CG}(u_h, u_h^P) + \int_0^T a_{DG}(u_h, u_h^H) = \int_0^T l_{CG}(u_h^P).$$

Use Lemma 3.2 to infer

$$(37) \quad |||u_h|||^2 = \frac{1}{2}\|u_h(0)\|_\Omega^2 + \int_0^T l_{CG}(u_h^P).$$

To bound the terms on the right-hand side with the given data, apply Young's inequality with $\delta = 2$ to obtain

$$(38) \quad -\langle \alpha \hat{g} \cdot n_{\partial\Omega}, u_h^P \rangle_F \leq \frac{1}{4} \langle |\alpha \cdot n_{\partial\Omega}|, (u_h^P)^2 \rangle_F + \langle |\alpha \cdot n_{\partial\Omega}|, \hat{g}^2 \rangle_F,$$

and hide the former term in the left hand side of equation (37). Finally, owing to (20), $\|u_h(0)\|_\Omega \leq \|u_0\|_\Omega$; the conclusion is straightforward. \square

Define the parabolic projection $\Pi^P u^P(\cdot, t) \in V_h^{\text{CG}}$ such that

$$(39) \quad \partial_t(\Pi^P u^P - u^P, w)_{\Omega_P} + (\nu \nabla(\Pi^P u^P - u^P), \nabla w)_{\Omega_P} = 0 \quad \forall w \in V_h^{\text{CG}},$$

with $\Pi^P u^P(\cdot, 0) = u_h^P(0)$. Let $\Pi^H u^H(\cdot, t) \in V_h^{\text{DG}}$ be the L^2 projection of u^H onto V_h^{DG} . Recall the following approximation result:

Lemma 3.4 (approximability). *Assume that the following constant is finite:*

$$(40) \quad C_* = \|u_0\|_{\Omega}^2 + \int_0^T \|u^P\|_{H^{p_{\text{CG}}+1}(\Omega_P)}^2 + \int_0^T \|u^H\|_{H^{p_{\text{DG}}+1}(\Omega_H)}^2.$$

Set $\theta^P = \Pi^P u - u^P$ and $\theta^H = \Pi^H u - u^H$. Let h_P and h_H be the maximum element diameter defined on Ω_P and Ω_H , respectively. Then, there is a constant $C_{*,a}$, independent of h_P, h_H but dependent on C_*, C_a , such that

$$(41) \quad \int_0^T \|\theta^P\|_{\Omega_P}^2 + h_P^2 \int_0^T \|\theta^P\|_{H^1(\Omega_P)}^2 \leq C_{*,a} h_P^{2p_{\text{CG}}+2},$$

$$(42) \quad \int_0^T \|\theta^H\|_{\Omega_H}^2 + h_H^2 \int_0^T \sum_{\Omega_e \in \mathcal{T}_h(\Omega_H)} \|\theta^H\|_{H^1(\Omega_e)}^2 \leq C_{*,a} h_H^{2p_{\text{DG}}+2}.$$

Collecting the results of Lemmas 3.1, 3.2, and 3.4 yields the following:

Theorem 3.5 (convergence). *Under the above assumptions, the scheme (19)-(20) satisfies the a priori error estimate*

$$(43) \quad |||u - u_h||| \leq C_{\alpha, \nu, t, i, *, a} \left(h_P^{2p_{\text{CG}}+1} + h_H^{2p_{\text{DG}}+1} \right)^{\frac{1}{2}},$$

where C is a constant independent of h_P, h_H but dependent on $\alpha, \nu, C_t, C_i, C_*$ and C_a .

Proof. Define $\eta^P = u_h^P - \Pi^P u^P$ and $\eta^H = u_h^H - \Pi^H u^H$. Set $\eta = (\eta^P, \eta^H)$ and $\theta = (\theta^P, \theta^H)$. Owing to Lemma 3.1, it is readily inferred that

$$(44) \quad \int_0^T a_{\text{CG}}(\eta, \eta^P) + \int_0^T a_{\text{DG}}(\eta, \eta^H) = \int_0^T a_{\text{CG}}(\theta, \eta^P) + \int_0^T a_{\text{DG}}(\theta, \eta^H).$$

From Lemma 3.2, the left hand side of the above equation can be written

$$(45) \quad \int_0^T a_{\text{CG}}(\eta, \eta^P) + \int_0^T a_{\text{DG}}(\eta, \eta^H) = |||\eta|||^2,$$

since $\eta(0) = 0$. Therefore, equation (44) becomes

$$(46) \quad \begin{aligned} |||\eta|||^2 &= - \int_0^T (\alpha \theta^P, \nabla \eta^P)_{\Omega_P} \\ &\quad - \int_0^T \sum_{\Omega_e \in \mathcal{T}_h(\Omega_H)} (\alpha \theta^H, \nabla \eta^H)_{\Omega_e} + \int_0^T \sum_{F \in F_H^i} \langle \alpha (\theta^H)^\dagger, [\eta^H] \rangle_F \\ &\quad - \int_0^T \sum_{F \in F_\Gamma^i} \langle \alpha \theta^\dagger \cdot n_\Gamma, \eta^P \rangle_F + \int_0^T \sum_{F \in F_\Gamma^i} \langle \alpha \theta^\dagger \cdot n_\Gamma, \eta^H \rangle_F \\ &\quad + \int_0^T \sum_{F \in F_{\text{out}}^\partial} \langle \alpha \theta^P \cdot n_{\partial\Omega}, \eta^P \rangle_F \\ &\equiv T_1 - T_6. \end{aligned}$$

We now bound each of the terms on the right hand side of this equation using Lemma 3.4. Using Cauchy-Schwartz and Young's inequality followed by approximation results, term one is bounded as

$$\begin{aligned}
-\int_0^T (\alpha \theta^P, \nabla \eta^P)_{\Omega_P} &\leq C_{\alpha, \nu} \int_0^T \|\theta^P\|_{\Omega_P} \|\nu^{\frac{1}{2}} \nabla \eta^P\|_{\Omega_P} \\
&\leq C_{\alpha, \nu, \delta} \int_0^T \|\theta^P\|_{\Omega_P}^2 + \delta \int_0^T \|\nu^{\frac{1}{2}} \nabla \eta^P\|_{\Omega_P}^2 \\
(47) \qquad \qquad \qquad &\leq C_{\alpha, \nu, \delta, *, a} h_P^{2p_{CG}+2} + \delta \int_0^T \|\nu^{\frac{1}{2}} \nabla \eta^P\|_{\Omega_P}^2.
\end{aligned}$$

To control term two, let $\Pi^0 \alpha$ be the L^2 -orthogonal projection of α onto element-wise constants in $\mathcal{T}_h(\Omega_H)$. Since $\alpha \in W_\infty^1(\Omega)$, $\|\Pi^0 \alpha - \alpha\|_{L^\infty(\Omega_e)} \leq C_\alpha h_H$ for all $\Omega_e \in \mathcal{T}_h(\Omega_H)$. By definition of θ^H , we can incorporate $\Pi^0 \alpha$ and apply inverse inequality (12) to obtain

$$\begin{aligned}
-\int_0^T \sum_{\Omega_e \in \mathcal{T}_h(\Omega_H)} (\alpha \theta^H, \nabla \eta^H)_{\Omega_e} &= \int_0^T \sum_{\Omega_e \in \mathcal{T}_h(\Omega_H)} ((\Pi^0 \alpha - \alpha) \theta^H, \nabla \eta^H)_{\Omega_e} \\
&\leq C_\alpha h_H \int_0^T \sum_{\Omega_e \in \mathcal{T}_h(\Omega_H)} \|\theta^H\|_{\Omega_e} \|\eta^H\|_{H^1(\Omega_e)} \\
(48) \qquad \qquad \qquad &\leq C_{\alpha, *, a} h_H^{2p_{DG}+2} + \int_0^T \|\eta^H\|_{\Omega_H}^2.
\end{aligned}$$

By inequalities (11) and (12), term three is bounded as

$$\begin{aligned}
&\int_0^T \sum_{F \in F_H^i} \langle \alpha (\theta^H)^\dagger, [\eta^H] \rangle_F \\
&\leq C_\delta \int_0^T \sum_{F \in F_H^i} \langle |\alpha \cdot n_F|, (\theta^H)^\dagger \rangle_F + \delta \int_0^T \sum_{F \in F_H^i} \langle |\alpha \cdot n_F|, [\eta^H]^2 \rangle_F \\
&\leq C_{\alpha, t, \delta} \int_0^T \sum_{\Omega_e \in \mathcal{T}_h(\Omega_H)} \|\theta^H\|_{\Omega_e} \|\theta^H\|_{H^1(\Omega_e)} + \delta \int_0^T \sum_{F \in F_H^i} \langle |\alpha \cdot n_F|, [\eta^H]^2 \rangle_F \\
(49) \qquad \qquad \qquad &\leq C_{\alpha, \delta, t, i, *, a} h_H^{2p_{DG}+1} + \delta \int_0^T \sum_{F \in F_H^i} \langle |\alpha \cdot n_F|, [\eta^H]^2 \rangle_F.
\end{aligned}$$

Similarly, terms four and five can be combined as

$$\begin{aligned}
&-\int_0^T \sum_{F \in F_\Gamma^i} \langle \alpha \theta^\dagger \cdot n_\Gamma, \eta^P \rangle_F + \int_0^T \sum_{F \in F_\Gamma^i} \langle \alpha \theta^\dagger \cdot n_\Gamma, \eta^H \rangle_F \\
&\leq C_\delta \int_0^T \sum_{F \in F_\Gamma^i} \langle |\alpha \cdot n_\Gamma|, (\theta^\dagger)^2 \rangle_F + \delta \int_0^T \sum_{F \in F_\Gamma^i} \langle |\alpha \cdot n_\Gamma|, (\eta^H - \eta^P)^2 \rangle_F \\
&\leq C_{\alpha, t, \delta} \int_0^T \sum_{\Omega_e \in \mathcal{T}_h} \|\theta\|_{\Omega_e} \|\theta\|_{H^1(\Omega_e)} + \delta \int_0^T \sum_{F \in F_\Gamma^i} \langle |\alpha \cdot n_\Gamma|, (\eta^H - \eta^P)^2 \rangle_F \\
(50) \qquad \qquad \qquad &\leq C_{\alpha, \delta, t, i, *, a} \left(h_H^{2p_{DG}+1} + h_P^{2p_{CG}+1} \right) + \delta \int_0^T \sum_{F \in F_\Gamma^i} \langle |\alpha \cdot n_\Gamma|, (\eta^H - \eta^P)^2 \rangle_F,
\end{aligned}$$

and term six as

$$\begin{aligned}
& \int_0^T \sum_{F \in F_{\text{out}}^\partial} \langle \alpha \theta^P \cdot n_{\partial\Omega}, \eta^P \rangle_F \\
& \leq C_{\alpha,t,\delta} \int_0^T \|\theta^P\|_{\Omega_P} \|\theta^P\|_{H^1(\Omega_P)} + \delta \int_0^T \sum_{F \in F_{\text{out}}^\partial} \langle |\alpha \cdot n_{\partial\Omega}|, (\eta^P)^2 \rangle_F \\
(51) \quad & \leq C_{\alpha,\delta,t,i,*,a} h_P^{2p_{\text{CG}}+1} + \delta \int_0^T \sum_{F \in F_{\text{out}}^\partial} \langle |\alpha \cdot n_{\partial\Omega}|, (\eta^P)^2 \rangle_F.
\end{aligned}$$

Incorporate each of these bounds into equation (46) to obtain

$$\begin{aligned}
\|\eta\|^2 & \leq C_{\alpha,\nu,\delta,t,i,*,a} \left(h_H^{2p_{\text{DG}}+1} + h_P^{2p_{\text{CG}}+1} \right) + \int_0^T \|\eta^H\|_{\Omega_H}^2 \\
& + \delta \int_0^T \|\nu^{\frac{1}{2}} \nabla \eta^P\|_{\Omega_P}^2 + \delta \int_0^T \sum_{F \in F_\Gamma^i} \langle |\alpha \cdot n_\Gamma|, (\eta^H - \eta^P)^2 \rangle_F \\
(52) \quad & + \delta \int_0^T \sum_{F \in F_H^i} \langle |\alpha \cdot n_F|, [\eta^H]^2 \rangle_F + \delta \int_0^T \sum_{F \in F_{\text{out}}^\partial} \langle |\alpha \cdot n_{\partial\Omega}|, (\eta^P)^2 \rangle_F.
\end{aligned}$$

Take δ sufficiently small to hide the corresponding terms in the right hand side, and apply Gronwall's Lemma. Application of the triangle inequality then yields the theorem. \square

Remark 3.6. *The polynomial degree p may vary element by element in the DG region; thus, in the a priori error estimate of Theorem 3.5, p_{DG} represents the lowest degree polynomial over all elements $\Omega_e \in \Omega_H$.*

3.3. Numerical Results. In this section we discuss numerical results for discretizations of the model hyperbolic-parabolic problem (1)-(8) by the coupled CG/DG method.

3.3.1. Test Case 1. To validate the convergence rates of our coupled formulation, we consider a one-dimensional test case with analytical solution. The domain $\Omega =]0, 2[$ is split into three distinct subdomains $\Omega = \Omega_{P1} \cup \Omega_H \cup \Omega_{P2}$ with $\Omega_{P1} =]0, 1[$, $\Omega_H =]1, 1.5[$, and $\Omega_{P2} =]1.5, 2[$. The diffusion coefficient is set to 1 on $\Omega_{P1} \cup \Omega_{P2}$ and vanishes on Ω_H . The advection velocity is set to 1 throughout the domain Ω . Hence, $\Gamma_{PH} = \{1\}$ and $\Gamma_{HP} = \{1.5\}$.

A non-zero right hand side f is added to equations (1)-(2). The data f , together with the initial condition u_0 and the inflow data \hat{g} , are chosen in such a way that the following function

$$(53) \quad u(x, t) = -\sin(x-1) + \exp(x-1) + (x-1)^2 t \quad \text{on } \Omega_{P1},$$

$$(54) \quad u(x, t) = (x-1)^2(1+t) + 1 \quad \text{on } \Omega_H,$$

$$(55) \quad u(x, t) = 1 + (x-1.5)(x^2 + a(t)x + b(t))t \quad \text{on } \Omega_{P2},$$

satisfies (1)-(4) for all $t \geq 0$. Moreover, this function matches the interface conditions (6)-(7) at the parabolic to hyperbolic interface Γ_{PH} . The time-dependent functions a and b are chosen so that on the one hand, the interface condition (8) is satisfied at the hyperbolic to parabolic interface Γ_{HP} and on the other hand, the outflow condition (5) holds at $\partial\Omega_{\text{out}} = \{2\}$. This yields $a(t) = \frac{t}{4} - \frac{7}{2}$ and

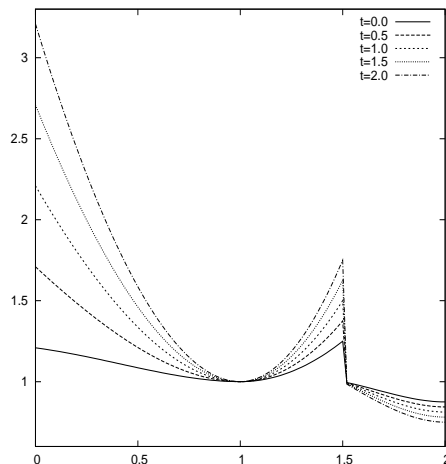


FIGURE 2. Test case 1: exact solution profiles at times $t = 0.0, 0.5, 1.0, 1.5$ and 2.0 .

h	Ω_{P1}		Ω_H		Ω_{P2}		Ω	
	L^2 error	rate	L^2 error	rate	L^2 error	rate	L^2 error	rate
1/8	0.005451		0.00827		0.001826		0.01555	
1/16	0.001363	2.00	0.00207	2.00	0.000458	1.99	0.00390	2.00
1/32	0.000341	2.00	0.00052	2.00	0.000110	2.05	0.00097	2.00
1/64	0.000085	2.00	0.00013	2.00	0.000028	1.98	0.00024	2.00

TABLE 1. Test case 1: convergence rates in each subdomain.

$b(t) = \frac{11}{4} - \frac{5t}{8}$. Figure 2 displays the time evolution of the exact solution profile at times $t = 0.0, 0.5, 1.0, 1.5$ and 2.0 .

We consider a CG discretization on $\Omega_{P1} \cup \Omega_{P2}$ coupled to a DG discretization on Ω_H . The bilinear form is defined by equations (16)-(17) and the discrete problem consists of solving equation (19) with a trivial modification resulting from the non-zero source term f . We consider a sequence of nested uniform grids. Linear basis functions are utilized in space and a simple Euler method in time without slope limiting. Table 1 lists the L^2 error and convergence rates for each subdomain and for the entire domain Ω . The convergence achieved numerically is one-half order higher than our theory predicts. These types of convergence results are similarly reflected in current research on DG methods in general.

3.3.2. Test Case 2. We consider the rectangular domain $]0, 2[\times]0, 1[$ with a triangular mesh consisting of 800 elements. In Figure 3 we display the hyperbolic subdomain

$$(56) \quad \Omega_H =]0.4, 0.6[\times]0.2, 1.0[\cup]1.4, 1.6[\times]0.2, 1.0[,$$

and the parabolic subdomain $\Omega_P = \Omega \setminus \Omega_H$ in which we set $\nu = 1.0$. The advection velocity is chosen to be $\alpha = (1.0, 0.0)^T$ so that

$$(57) \quad \Gamma_{PH} = \{0.4\} \times]0.2, 1.0[\cup \{1.4\} \times]0.2, 1.0[,$$

$$(58) \quad \Gamma_{HP} = \{0.6\} \times]0.2, 1.0[\cup \{1.6\} \times]0.2, 1.0[.$$

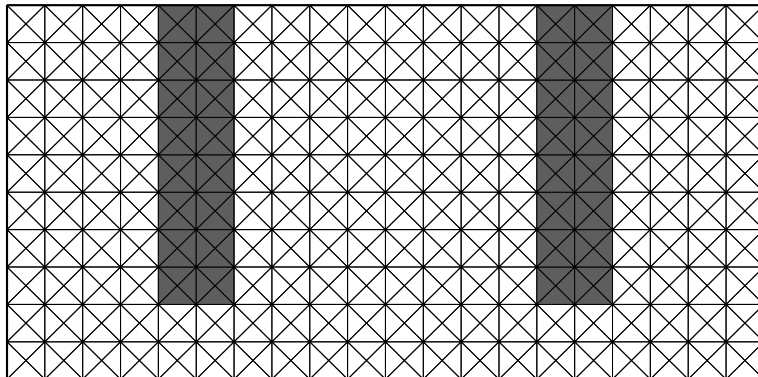


FIGURE 3. Test case 2: Mesh and domain partition of hyperbolic subdomain Ω_H (dark) and parabolic subdomain Ω_P (light).

We impose no-flow boundaries on the top and bottom, inflow on the left (with $\hat{g} = 1$ at all times) and outflow on the right boundaries of Ω . The initial solution consists of $u = 0$ everywhere in the domain. Thus, the model problem mimics the propagation of a wave from the left to the right boundary as it progresses through parabolic and diffusion-degenerate subdomains.

We employ a DG discretization in the hyperbolic domain and a CG method in the parabolic domain as defined in equations (16)-(17). The time discretization is accomplished via a simple explicit Euler method without slope limiting. The time step limitation is the usual one for this kind of problems, namely $\delta t \leq ch^2$ where h is the mesh size. The contour lines of the discrete solution at times $t = .5, 1.0, 1.5$ and 2.0 are displayed in Figure 4. The same gray-color scale spanning values between 0 and 1 is used for the four plots. The discontinuities of the solution across Γ_{HP} are clearly visible. We also observe that the contour lines in Ω_P tend to be perpendicular to Γ_{PH} , indicating that the homogeneous Neumann outflow condition approximately holds on Γ_{PH} as predicted by the theory.

Figure 5 displays the time evolution of the solution profile along the line $y = 0.55$. The propagation of the wave from the left to the right is clearly illustrated. Note that at the parabolic to hyperbolic interface Γ_{PH} the solution is continuous though not C^1 in agreement with theoretical results [8, 9]. Furthermore, the solution is discontinuous on the hyperbolic to parabolic interface Γ_{HP} .

4. Coupled NIPG/DG formulation

In this section we formulate the coupling of the NIPG method discretizing the parabolic equation (1) on Ω_P with the DG method discretizing the hyperbolic equation (2) on Ω_H . Then, we analyze the coupled discrete scheme and present some numerical results. We emphasize the importance of imposing interface conditions on Γ that are consistent with (6)-(8).

4.1. The scheme. Let p_{NIPG} be a positive integer and set

$$(59) \quad V_h^{\text{NIPG}} = \{v \in L^2(\Omega_P) : \forall \Omega_e \in \mathcal{T}_h(\Omega_P), v|_{\Omega_e} \in \mathbb{P}^{p_{\text{NIPG}}}(\Omega_e)\}.$$

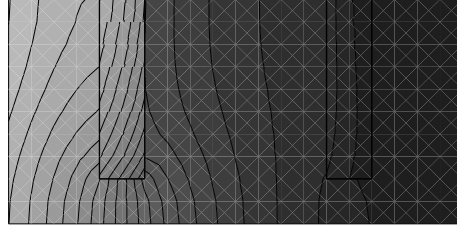
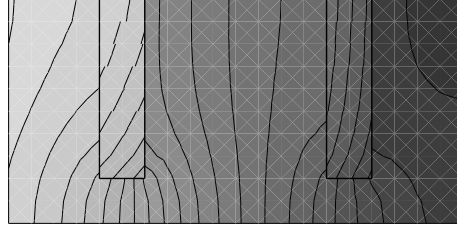
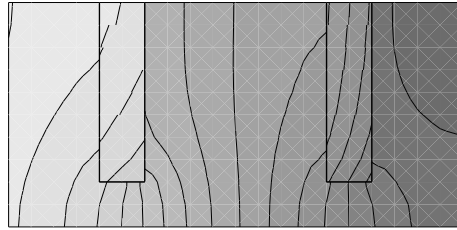
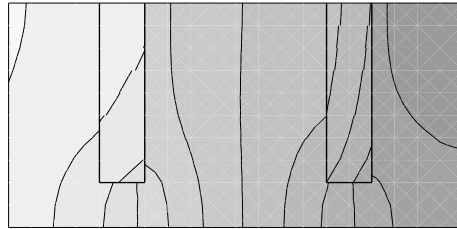

 (a) solution at $t = 0.5$

 (b) solution at $t = 1.0$

 (c) solution at $t = 1.5$

 (d) solution at $t = 2.0$

 FIGURE 4. Test case 2: coupled CG/DG method solution contour lines at times $t = .5, 1.0, 1.5$ and 2.0 .

For a smooth enough function ψ , set $\psi^P = \psi|_{\Omega_P}$ and $\psi^H = \psi|_{\Omega_H}$. For a test function $w_h \in V_h^{\text{NIPG}}$, define the bilinear form

$$\begin{aligned}
 a_{\text{NIPG}}(\psi, w_h) &= (\partial_t \psi^P, w_h)_{\Omega_P} - \sum_{\Omega_e \in \mathcal{T}_h(\Omega_P)} (\alpha \psi^P - \nu \nabla \psi^P, \nabla w_h)_{\Omega_e} \\
 &+ \sum_{F \in F_P^i} \varsigma_F \langle \psi^P, w_h \rangle + \sum_{F \in F_\Gamma^i} \iota_F \langle \psi, w_h \rangle \\
 &+ \sum_{F \in F_P^i} \langle \alpha (\psi^P)^\dagger, [w_h] \rangle_F + \sum_{F \in F_{\text{out}}^\partial} \langle \alpha \psi^P \cdot n_{\partial\Omega}, w_h \rangle_F,
 \end{aligned}
 \tag{60}$$

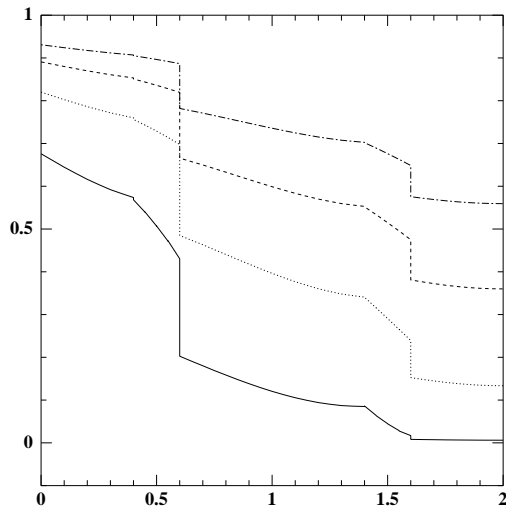


FIGURE 5. Test case 2: coupled CG/DG method solution profiles along the line $y = 0.55$ at times $t = .5, 1.0, 1.5$ and 2.0 .

and the linear form

$$(61) \quad l_{\text{NIPG}}(w_h) = - \sum_{F \in F_{\text{in}}^{\partial}} \langle \alpha \hat{g} \cdot n_{\partial\Omega}, w_h \rangle_F.$$

Here, $\varsigma_F \langle \psi^P, w_h \rangle$ denotes the standard non-symmetric interior penalty term

$$(62) \quad \varsigma_F \langle \psi^P, w_h \rangle = - \langle \{\nu \nabla \psi^P\}, [w_h] \rangle_F + \langle \{\nu \nabla w_h\}, [\psi^P] \rangle_F + \langle \sigma_F [\psi^P], [w_h] \rangle_F,$$

with parameter

$$(63) \quad \sigma_F = \nu \sigma_0 |F|^{-\beta},$$

where σ_0 is a positive constant and $|F|$ is the $(d-1)$ -dimensional measure of F . Moreover, $\sum_{F \in F_{\Gamma}^i} \iota_F \langle \psi, w_h \rangle$ collects the interface terms on Γ . We consider two approaches to define those terms, namely

$$(64) \quad \iota_F^* \langle \psi, w_h \rangle = \langle \alpha \psi^{\uparrow} \cdot n_{\Gamma}, w_h \rangle_F,$$

$$(65) \quad \iota_F^{\diamond} \langle \psi, w_h \rangle = \langle \alpha \psi^{\uparrow} \cdot n_{\Gamma}, w_h \rangle_F + \varsigma_F \langle \psi, w_h \rangle.$$

Here, $\iota_F^* \langle \psi, w_h \rangle$ incorporates the continuity restrictions (6)-(8) on the interface boundary terms, while $\iota_F^{\diamond} \langle \psi, w_h \rangle$ results from a straightforward NIPG method discretization with the standard assumption of continuity of the flux and solution on the interface. The coupled NIPG/DG scheme is then formulated as follows: Seek $u_h = (u_h^P, u_h^H) \in C^1([0, T]; V_h^{\text{NIPG}} \times V_h^{\text{DG}})$ such that, for all $t > 0$ and for all $(w_h, v_h) \in V_h^{\text{NIPG}} \times V_h^{\text{DG}}$,

$$(66) \quad a_{\text{NIPG}}(u_h, w_h) + a_{\text{DG}}(u_h, v_h) = l_{\text{NIPG}}(w_h),$$

with interface terms defined by either (64) or (65). The initial condition is the L^2 -orthogonal projection of u_0 onto $V_h^{\text{NIPG}} \times V_h^{\text{DG}}$.

4.2. Analysis. As for the coupled CG/DG scheme, the convergence analysis for the coupled NIPG/DG scheme relies on consistency and stability properties. A straightforward verification yields the following:

Lemma 4.1 (consistency). *Assume that u is a strong solution of (1)-(8). Then, if the interface terms are evaluated as in (64),*

$$(67) \quad a_{\text{NIPG}}(u, w_h) + a_{\text{DG}}(u, v_h) = l_{\text{NIPG}}(w_h) \quad \forall (w_h, v_h) \in V_h^{\text{NIPG}} \times V_h^{\text{DG}}.$$

If the interface terms are evaluated as in (65), the scheme suffers from a lack of consistency. For $F \in \Gamma_{\text{PH}}$, the exact solution u is continuous and $\{\nu \nabla u\} = 0$ owing to (6)-(7); hence, $\varsigma_F(u, w_h) = 0$ and consistency is recovered. However, for $F \in \Gamma_{\text{HP}}$, the exact solution is discontinuous implying that $\varsigma_F(u, w_h) \neq 0$ in general.

To establish a stability estimate, modify the definition of the triple norm as follows:

$$(68) \quad \begin{aligned} |||\psi|||^2 &\equiv \frac{1}{2} \|\psi(T)\|_{\Omega}^2 + \int_0^T \sum_{\Omega_e \in \mathcal{T}_h(\Omega_{\text{F}})} \|\nu^{\frac{1}{2}} \nabla \psi^{\text{P}}\|_{\Omega_e}^2 + \int_0^T \sum_{F \in F_{\text{P}}^{\text{i}}} \|\sigma_F^{\frac{1}{2}} [\psi^{\text{P}}]\|_F^2 \\ &\quad + \frac{1}{2} \int_0^T \sum_{F \in F_{\text{out}}^{\text{o}}} \langle |\alpha \cdot n_{\partial\Omega}|, (\psi^{\text{P}})^2 \rangle_F + \frac{1}{2} \int_0^T \sum_{F \in F_{\text{in}}^{\text{o}}} \langle |\alpha \cdot n_{\partial\Omega}|, (\psi^{\text{P}})^2 \rangle_F \\ &\quad + \frac{1}{2} \int_0^T \sum_{F \in F_{\text{P}}^{\text{i}}} \langle |\alpha \cdot n_F|, [\psi^{\text{P}}]^2 \rangle_F + \frac{1}{2} \int_0^T \sum_{F \in F_{\text{H}}^{\text{i}}} \langle |\alpha \cdot n_F|, [\psi^{\text{H}}]^2 \rangle_F \\ &\quad + \frac{1}{2} \int_0^T \sum_{F \in F_{\Gamma}^{\text{i}}} \langle |\alpha \cdot n_{\Gamma}|, [\psi]^2 \rangle_F. \end{aligned}$$

Proceeding similarly to the proof of Lemma 3.2 and Corollary 3.3 readily yields the following:

Lemma 4.2 (stability). *For all $v_h = (v_h^{\text{P}}, v_h^{\text{H}}) \in V_h^{\text{NIPG}} \times V_h^{\text{DG}}$,*

$$(69) \quad \int_0^T a_{\text{NIPG}}(v_h, v_h^{\text{P}}) + \int_0^T a_{\text{DG}}(v_h, v_h^{\text{H}}) = |||v_h|||^2 - \frac{1}{2} \|v_h(0)\|_{\Omega}^2.$$

Corollary 4.3. *The scheme (66) satisfies the stability result*

$$(70) \quad |||u_h|||^2 \leq \|u_0\|_{\Omega}^2 + 2 \int_0^T \sum_{F \in F_{\text{in}}^{\text{o}}} \langle |\alpha \cdot n_{\partial\Omega}|, \hat{g}^2 \rangle_F.$$

Theorem 4.4 (convergence). *Assume that the following constant is finite:*

$$(71) \quad C_* = \|u_0\|_{\Omega}^2 + \int_0^T \|u^{\text{P}}\|_{H^{p_{\text{NIPG}}+1}(\Omega_{\text{F}})}^2 + \int_0^T \|\partial_t u^{\text{P}}\|_{H^{p_{\text{NIPG}}+1}(\Omega_{\text{F}})}^2 + \int_0^T \|u^{\text{H}}\|_{H^{p_{\text{DG}}+1}(\Omega_{\text{H}})}^2.$$

Set $f = \partial_t u^{\text{P}} + \nabla \cdot (\alpha u^{\text{P}})$ and assume that for a.e. $t \geq 0$, f and its time-derivative are in $L^2(\Omega_{\text{P}})$. Set $q = \alpha(u^{\text{P}} - \hat{g})$ for $x \in \partial\Omega_{\text{in}}$, $q = 0$ for $x \in \partial\Omega_{\text{out}} \cup \partial\Omega_0$, and $q = \alpha(u^{\text{P}} - u^{\text{H}})$ for $x \in \Gamma$ and assume that for a.e. $t \geq 0$, q and its time-derivative are in $L^2(\partial\Omega_{\text{P}})$. Assume that the PDE (1) holds at $t = 0$. Choose parameter β in (63) such that $\beta \geq 3$ for $d = 2$ and $\beta \geq \frac{3}{2}$ for $d = 3$. Then, the scheme (66) with interface terms defined in (64) satisfies the a priori error estimate

$$(72) \quad |||u - u_h||| \leq C_{\alpha, \nu, \delta, t, i, \beta, \sigma_0, *, a} \left(h_{\text{P}}^{2p_{\text{NIPG}} - 2 + \beta(d-1)} + h_{\text{H}}^{2p_{\text{DG}} + 1} \right)^{\frac{1}{2}}$$

where C is a constant independent of h_P, h_H but dependent on $\alpha, \nu, \sigma_0, \beta, C_*, C_t, C_i$ and C_a .

Proof. The main idea is to recast our model problem (1) in the parabolic domain into an elliptic format at a fixed time and to use the results by Rivière, Wheeler and Girault [7] for the NIPG method applied to elliptic problems.

(i) Set $f = \partial_t u^P + \nabla \cdot (\alpha u^P)$ and set $q = \alpha(u^P - \hat{g})$ for $x \in \partial\Omega_{\text{in}}$, $q = 0$ for $x \in \partial\Omega_{\text{out}} \cup \partial\Omega_0$, and $q = \alpha(u^P - u^H)$ for $x \in \Gamma$. Consider the elliptic problem

$$(73) \quad -\nabla \cdot (\nu \nabla \phi) = f, \quad x \in \Omega_P,$$

$$(74) \quad \nu \nabla \phi \cdot n_{\partial\Omega} = q \cdot n_{\partial\Omega}, \quad x \in \partial\Omega_P.$$

Owing to the above assumptions, its solution is $\phi = u^P$. Similarly, the above assumptions imply that $\partial_t u^P$ is the exact solution of the elliptic problem (73)-(74) in which f and q are replaced by their time-derivatives. Now define $\phi_h \in V_h^{\text{NIPG}}$ to be such that for all $w_h \in V_h^{\text{NIPG}}$,

$$(75) \quad \begin{aligned} & \sum_{\Omega_e \in \mathcal{T}_h(\Omega_P)} (\nu \nabla \phi_h, \nabla w_h)_{\Omega_e} + \sum_{F \in F_P^i} \varsigma_F \langle \phi_h, w_h \rangle \\ &= \sum_{\Omega_e \in \mathcal{T}_h(\Omega_P)} (f, w_h)_{\Omega_e} + \sum_{F \in F_{\text{in}}^{\partial}} \langle q \cdot n_{\partial\Omega}, w_h \rangle_F + \sum_{F \in F_{\Gamma}^i} \langle q \cdot n_{\Gamma}, w_h \rangle_F. \end{aligned}$$

Under the above assumptions on the data, the scheme (75) is consistent with the elliptic problem (73)-(74). Furthermore, if ν is sufficiently smooth such that the solution of the elliptic dual problem belongs to $H^2(\Omega_P)$ with continuous dependence on f and q , then the following results hold [7] :

$$(76) \quad \|\phi_h - \phi\|_{\Omega_P} \leq C_{\beta} h_P^{p_{\text{NIPG}} - \frac{1}{2} + \frac{\beta}{2}(d-1)} \sum_{\Omega_e \in \mathcal{T}_h(\Omega_P)} \|\phi\|_{H^{p_{\text{NIPG}}+1}(\Omega_e)},$$

for C_{β} independent of h_P and ϕ , and

$$(77) \quad \sum_{\Omega_e \in \mathcal{T}_h(\Omega_P)} \|\nu^{\frac{1}{2}} \nabla(\phi_h - \phi)\|_{\Omega_e} \leq C_{\beta, \nu, \sigma} h_P^{p_{\text{NIPG}}} \sum_{\Omega_e \in \mathcal{T}_h(\Omega_P)} \|\phi\|_{H^{p_{\text{NIPG}}+1}(\Omega_e)},$$

for $C_{\beta, \nu, \sigma}$ independent of h_P and ϕ . As a result, setting $\theta^P = u^P - \phi_h$ yields

$$(78) \quad \begin{aligned} & \int_0^T \|\theta^P\|_{\Omega_P}^2 + h_P^2 \int_0^T \sum_{\Omega_e \in \mathcal{T}_h(\Omega_P)} \|\theta^P\|_{H^1(\Omega_e)}^2 + \int_0^T \|\partial_t \theta^P\|_{H^s(\Omega_P)}^2 \\ & \leq C_{*, \beta, \nu} h_P^{2p_{\text{NIPG}} - 1 + \beta(d-1)}. \end{aligned}$$

(ii) Set $\eta^P = u_h^P - \phi_h$ and $\eta^H = u_h^H - \Pi^H u$ for $\Pi^H u \in V_h^{\text{DG}}$ the L^2 -orthogonal projection of u^H onto V_h^{DG} . Define $\eta = (\eta^P, \eta^H)$. Let $\theta^H = u^H - \Pi^H u$ and define $\theta = (\theta^P, \theta^H)$ with θ^P defined above. Note that $\eta(0) = 0$. On Ω_H , this fact directly results from the construction of $\eta^H(0)$ while on Ω_P , it results from the assumption that the PDE (1) holds initially. Owing to Lemma 4.1, it is readily inferred that

$$(79) \quad \int_0^T a_{\text{NIPG}}(\eta, \eta^P) + \int_0^T a_{\text{DG}}(\eta, \eta^H) = \int_0^T a_{\text{NIPG}}(\theta, \eta^P) + \int_0^T a_{\text{DG}}(\theta, \eta^H).$$

Using (75) yields

$$\begin{aligned}
\int_0^T a_{\text{NIPG}}(\theta, \eta^{\text{P}}) &= \int_0^T (\partial_t \theta^{\text{P}}, \eta^{\text{P}})_{\Omega_{\text{P}}} - \int_0^T \sum_{\Omega_e \in \mathcal{T}_h(\Omega_{\text{P}})} (\alpha \theta^{\text{P}}, \nabla \eta^{\text{P}})_{\Omega_e} \\
&+ \int_0^T \sum_{F \in F_{\text{P}}^i} \langle \alpha (\theta^{\text{P}})^\dagger, [\eta^{\text{P}}] \rangle_F + \int_0^T \sum_{F \in F_{\Gamma}^i} \langle \alpha \theta^\dagger \cdot n_{\Gamma}, \eta^{\text{P}} \rangle_F \\
(80) \quad &+ \int_0^T \sum_{F \in F_{\text{out}}^\partial} \langle \alpha \theta^{\text{P}} \cdot n_{\partial\Omega}, \eta^{\text{P}} \rangle_F.
\end{aligned}$$

From Lemma 4.2, the left hand side of equation (79) can be written

$$(81) \quad \int_0^T a_{\text{NIPG}}(\eta, \eta^{\text{P}}) + \int_0^T a_{\text{DG}}(\eta, \eta^{\text{H}}) = \|\eta\|^2,$$

since $\eta(0) = 0$. Therefore, equation (79) becomes

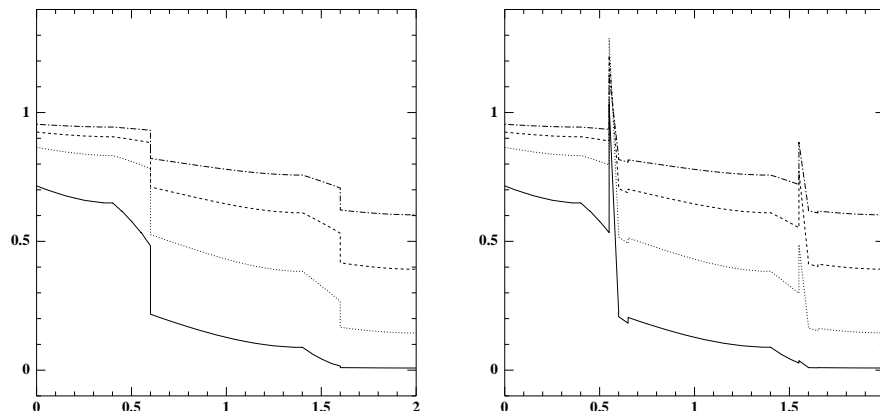
$$\begin{aligned}
\|\eta\|^2 &= - \int_0^T \sum_{\Omega_e \in \mathcal{T}_h(\Omega_{\text{H}})} (\alpha \theta^{\text{H}}, \nabla \eta^{\text{H}})_{\Omega_e} + \int_0^T \sum_{F \in F_{\text{H}}^i} \langle \alpha (\theta^{\text{H}})^\dagger, [\eta^{\text{H}}] \rangle_F \\
&+ \int_0^T \sum_{F \in F_{\Gamma}^i} \langle \alpha \theta^\dagger \cdot n_{\Gamma}, \eta^{\text{H}} \rangle_F + \int_0^T (\partial_t \theta^{\text{P}}, \eta^{\text{P}})_{\Omega_{\text{P}}} \\
&- \int_0^T \sum_{\Omega_e \in \mathcal{T}_h(\Omega_{\text{P}})} (\alpha \theta^{\text{P}}, \nabla \eta^{\text{P}})_{\Omega_e} + \int_0^T \sum_{F \in F_{\text{P}}^i} \langle \alpha (\theta^{\text{P}})^\dagger, [\eta^{\text{P}}] \rangle_F \\
&- \int_0^T \sum_{F \in F_{\Gamma}^i} \langle \alpha \theta^\dagger \cdot n_{\Gamma}, \eta^{\text{P}} \rangle_F + \int_0^T \sum_{F \in F_{\text{out}}^\partial} \langle \alpha \theta^{\text{P}} \cdot n_{\partial\Omega}, \eta^{\text{P}} \rangle_F \\
(82) \quad &\equiv T_1 - T_8.
\end{aligned}$$

(iii) We now bound each of the terms on the right hand side of this equation using Lemma 3.4 and the approximability result. Term T_1 is handled as in the proof of Theorem 3.5, as is term T_2 with term T_6 bounded in a similar manner. Term T_3 is combined with T_7 as per equation (50). The fourth term can be easily bounded as

$$(83) \quad \int_0^T (\partial_t \theta^{\text{P}}, \eta^{\text{P}})_{\Omega_{\text{P}}} \leq \int_0^T C_{*,\beta} h_{\text{P}}^{2p_{\text{NIPG}}-1+\beta(d-1)} + \int_0^T \|\eta^{\text{P}}\|_{\Omega_{\text{P}}}^2.$$

Term T_5 is bounded similar to equation (47) in Theorem 3.5, and term T_8 similar to (51) using approximation (78). Incorporating each of these results yields

$$\begin{aligned}
\|\eta^{\text{P}}, \eta^{\text{H}}\|^2 &\leq C_{\alpha,\nu,\delta,t,i,\beta,\sigma_0,*} h_{\text{P}}^{2p_{\text{NIPG}}-2+\beta(d-1)} + C_{\alpha,\nu,\delta,t,i,*,a} h_{\text{H}}^{2p_{\text{DG}}+1} \\
&+ \int_0^T \|\eta^{\text{P}}\|_{\Omega_{\text{P}}}^2 + \int_0^T \|\eta^{\text{H}}\|_{\Omega_{\text{H}}}^2 + \delta \int_0^T \sum_{\Omega_e \in \mathcal{T}_h(\Omega_{\text{P}})} \|\nu^{\frac{1}{2}} \nabla \eta^{\text{P}}\|_{\Omega_e}^2 \\
&+ \delta \int_0^T \sum_{F \in F_{\Gamma}^i} \langle |\alpha \cdot n_{\Gamma}|, (\eta^{\text{H}} - \eta^{\text{P}})^2 \rangle_F + \delta \int_0^T \sum_{F \in F_{\text{P}}^i} \langle |\alpha \cdot n_F|, [\eta^{\text{P}}]^2 \rangle_F \\
(84) \quad &+ \delta \int_0^T \sum_{F \in F_{\text{H}}^i} \langle |\alpha \cdot n_F|, [\eta^{\text{H}}]^2 \rangle_F + \delta \int_0^T \sum_{F \in F_{\text{out}}^\partial} \langle |\alpha \cdot n_{\partial\Omega}|, (\eta^{\text{P}})^2 \rangle_F.
\end{aligned}$$



(a) Results for correct interface assumption (64) (b) Results for incorrect interface assumption (65)

FIGURE 6. NIPG/DG scheme: solution profiles along the line $y = 0.55$ at times $t = .5, 1.0, 1.5$ and 2.0 .

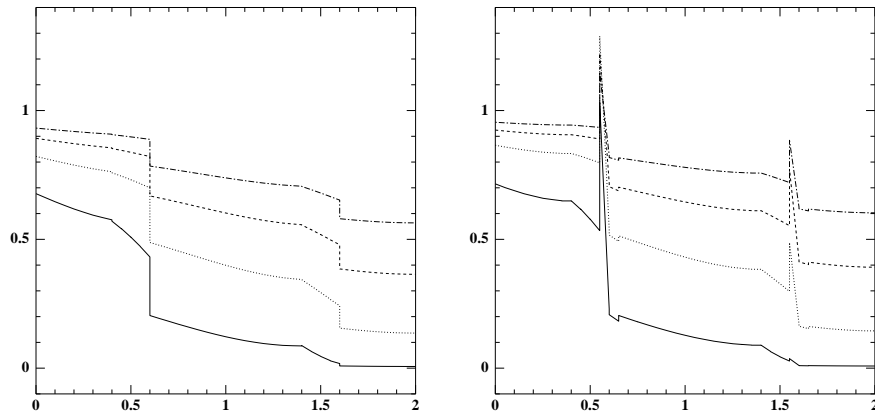
Take δ sufficient small to hide the corresponding terms in the right hand side, and apply Gronwall's Lemma. Application of the triangle inequality then yields the theorem. \square

Remark 4.5. A natural choice for parameter β in (63) is to choose $\beta = \frac{3}{a-1}$ in which case the convergence result of Theorem 4.4 matches the order of approximation proved in the CG/DG result.

4.3. Numerical Results. In this section we discuss numerical results for two-dimensional discretizations of the model hyperbolic-parabolic problem (1)-(8) by the coupled NIPG/DG method. The model problem considered here is the same as that of Section 3.3.2. We emphasize the importance of imposing the appropriate interface conditions in the definition of the method; in particular, we show that the DG scheme discretized without attention to the lack of regularity in the solution from the hyperbolic to parabolic subdomain results in the formation of a boundary layer at the interface. Recall that the “correct” coupled NIPG/DG scheme uses interface continuity restrictions (64), while the “incorrect” coupled NIPG/DG scheme naively incorporates faulty interface assumptions (65).

Figure 6 displays the solution profiles for both the correct and the incorrect NIPG/DG discretizations at times $t = .5, 1.0, 1.5$ and 2.0 . Note the presence of spurious oscillations at the interface between hyperbolic and parabolic regions Γ_{HP} in the latter scheme indicating an under-resolved boundary layer. The enforcement in the correct scheme of the appropriate interface restrictions results in solution profiles that are similar to those obtained with the coupled CG/DG scheme. This is in stark contrast to an approach that does not utilize the theoretical results and erroneously assumes continuity of both the solution and the flux in the discretization.

We also demonstrate that the enforcement of the theoretical interface conditions can be important even in the case of a non-degenerate diffusion coefficient if the local Peclet number in an advection-dominated subdomain is sufficiently high



(a) Results for correct interface assumption, $\nu = .001$ in Ω_H
 (b) Results for incorrect interface assumption, $\nu = .001$ in Ω_H

FIGURE 7. NIPG/DG scheme: solution profiles along the line $y = 0.55$ at times $t = .5, 1.0, 1.5$ and 2.0 .

to impose hyperbolic-type behavior in the solution. Suppose the problem is parabolic everywhere on the domain with a spatially dependent diffusion coefficient $\nu = \nu(x)$. Let $\nu = 1.0$ in subdomain Ω_P and $\nu = .001$ in subdomain Ω_H with an NIPG discretization of the parabolic equation (1) everywhere on Ω . Figure 7 displays the solution profiles for both a “correct” discretization incorporating interface restrictions (6)-(8) at the boundary where ν jumps in value, and an “incorrect” discretization.

5. Conclusions

Two coupled Galerkin methods applied to a model hyperbolic-parabolic problem were presented in this paper: a coupled CG/DG method and a coupled NIPG/DG method. Stability and *a priori* error estimates of order $h^{p+\frac{1}{2}}$ were derived. Numerical results demonstrate the importance of utilizing correct conditions at the interface, even for the case of a purely parabolic variable diffusion problem at high Peclet numbers. The multi-algorithmic approach presented herein should be particularly useful for the treatment of spatially varying or degenerate diffusion equations in which an adaptive computational scheme can be proposed. In such a scenario, the behavior of the exact solution as well as that of the approximate solution needs to be carefully considered when defining interface conditions between the algorithmic subdomains.

Acknowledgments

The authors thank Dr. Clint Dawson for valuable discussions.

References

- [1] C. Bernardi, Y. Maday and A.T. Patera, “A new nonconforming approach to domain decomposition: the mortar finite element method”, In *Nonlinear Partial Differential Equations and Their Applications*, H. Brezis and J.L.Lions, eds., Longman Scientific Technical, UK, 1994.
- [2] F.B. Belgacem, “The mortar finite element method with Lagrange multipliers”, *Numer. Math.*, 84:2, pp. 173–197, 1999.

- [3] M. Wheeler and I. Yotov, “Physical and computational domain decomposition for modeling subsurface flows”, *Contemp. Math.*, 218, pp. 217–228, 1998.
- [4] M. Peszynska, M. Wheeler and I. Yotov, “Mortar upscaling for multiphase flow in porous media”, *Comp. Geo.*, 6:1, pp. 73–100, 2002.
- [5] B. Cockburn and C. W. Shu, “The local discontinuous Galerkin finite element method for convection-diffusion systems”, *SIAM J. Num. Anal.*, 35, pp. 2440–2463, 1998.
- [6] J. T. Oden, I. Babuska and C. E. Baumann, “A discontinuous hp finite element method for diffusion problems”, *J. Comput. Phys.*, 146, pp. 491–516, 1998.
- [7] B. Rivière, M. F. Wheeler and V. Girault, “A priori error estimates for finite element methods based on discontinuous approximation spaces for elliptic problems”, *SIAM J. Numer. Anal.*, 39(3), pp. 902–931, 2001.
- [8] F. Gastaldi and A. Quarteroni, “On the coupling of hyperbolic and parabolic systems: Analytical and numerical approach”, *Appl. Numer. Math.*, 6, pp. 3–31, 1989.
- [9] J.-P. Croisille, A. Ern, T. Lelièvre and J. Proft, “Analysis and simulation of a coupled hyperbolic/parabolic model problem”, *J. Numer. Math.*, to appear 2004.
- [10] S.C. Brenner and L.R. Scott, *The Mathematical Theory of finite Element Methods*, Texts in Applied Mathematics Vol. 15, Springer-Verlag, New York, 1984.
- [11] A. Ern and J.-L. Guermond, *Theory and Practice of Finite Elements*, Applied Mathematical Series Vol. 159, Springer-Verlag, New York, 2004.

CERMICS, Ecole nationale des ponts et chaussées, 6/8 avenue Blaise Pascal, Champs sur Marne, F-77455 Marne-la-Vallée cedex 2, France

E-mail: ern@cermics.enpc.fr

LAMA, CNRS UMR 8050, Université Marne-la-Vallée, Champs sur Marne, F-77454 Marne-la-Vallée cedex 2, France

E-mail: proft@cermics.enpc.fr